ION CURRENT SATURATION ON ELECTRIC PROBES IN PLASMA FLOWS AT LOW REYNOLDS NUMBERS

Z. M. Egorova, A. V. Kashevarov, and N. S. Tskhai

UDC 533.9.082.76

Ion saturation currents are widely employed in the diagnostics of plasma of a continuous medium with the help of electric probes for determining the density of charged particles from the I–V curve of the probe [1]. The general expressions obtained in [1] for the saturation current densities permit deriving concrete diagnostic formulas for different regimes of plasma flow. Thus in [2] the ion saturation current on cylindrical and spherical probes in flows of incompressible plasma at quite high Reynolds numbers Re, when the flow at the surface of the probe occurs in the boundary-layer regime, was calculated. In [3] the saturation current at Re less than unity was determined.

An important plasma flow regime when performing probe measurements is flow at low Re (of the order of unity). This occurs, for example, in the study of ionization of laboratory flames with cylindrical and spherical probes with small diameter. In [4] analytical expressions are presented for the ion saturation current on a cylindrical probe under such conditions in some model cases of the velocity distribution of the ionized gas. The purpose of this work is to determine the saturation current on cylindrical and spherical probes at low Re taking into account the real viscous gas flow around the probes, obtained based on the solution of the Navier–Stokes equations.

1. We shall study the flow of an incompressible, thermodynamic equilibrium, weakly ionized plasma with constant transport properties and frozen chemical reactions near an infinitely long, conducting, cylindrical body (probe), whose symmetry axis is perpendicular to the velocity of the incident flow. According to the theory of [1] the saturation ion current is determined from the solution of the equation for the density of charged particles in the quasineutral region, which in polar coordinates (r, θ) can be written in the form

$$\frac{\partial^2 n}{\partial r^2}+\frac{1}{r}\frac{\partial n}{\partial r}+\frac{1}{r^2}\frac{\partial^2 n}{\partial \theta^2}-\frac{\mathrm{Re}_e}{2}\left(u_r\frac{\partial n}{\partial r}+u_\theta\frac{1}{r}\frac{\partial n}{\partial r}\right)=0. \quad (1.1)$$

Here $\mathrm{Re}_e = U_\infty R/D_i$ is the electric Reynolds number; U_∞ is the velocity of the incident flow; R is the radius of the probe; D_1 is the diffusion coefficient of the ions; μ_r and μ_θ are the radial and transverse velocities scaled to U_∞. The charged particle density is scaled to its value at infinity and the radial coordinate r is scaled to the radius of the probe.

The boundary conditions for Eq. (1.1) are

$$n|_{r=1}=0,\ n|_{r\to\infty}\to 1. \quad (1.2)$$

The dimensionless density of the saturation ion current is given by the expression

$$j=2\frac{\partial n}{\partial r}\Big|_{r=1}. \quad (1.3)$$

The field of the velocities u_r and u_θ is found from the solution of the problem of viscous fluid flow around the probe neglecting ionization.

2. The problem (1.1)-(1.3) was solved numerically. First the distribution of the velocities u_r and u_θ of viscous fluid flow around a circular cylinder was calculated by the

Zhukovskii. Translated from Zhurnal Prikladnoi Mekhaniki i Tekhnicheskoi Fiziki, No. 1, pp. 159-163, January-February, 1990. Original article submitted November 10, 1988.

 0021-8944/90/3101-0146$12.50

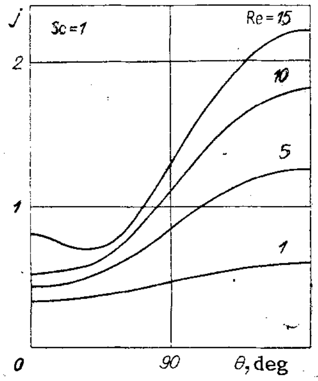

Fig. 1

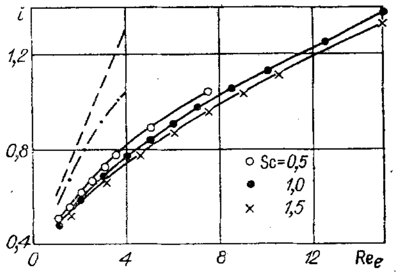

Fig. 2

method of [5, 6] for solving the Navier–Stokes equations. The calculation of the charged-particle density distribution was performed analogously.

The partial differential equation (1.1) was replaced by a finite-difference equation using an explicit five-point scheme. Since the density of charged particles changes most rapidly near the surface of the cylinder and since in solving the finite-difference problem it is desirable to have near the cylinder a more dense grid than far away from the cylinder the transformation $z = \ln r$ was first made in Eq. (1.1). Then Eq. (1.1) assumes the form

$$\frac{\partial^2 n}{\partial z^2}+\frac{\partial^2 n}{\partial \theta^2}-\frac{\mathrm{Re}_e}{2}\exp z\left(u_r\frac{\partial n}{\partial z}+u_\theta\frac{\partial n}{\partial \theta}\right)=0. \qquad (2.1)$$

The finite-difference approximation of Eq. (2.1) was made using central differences. The condition (1.2) at infinity was transferred to a circle with a quite large radius.

The finite-difference problem was solved by the method of successive approximations. The density distribution in the model case of the velocity field of a uniform undisturbed flow was taken as the zeroth approximation [4]. A grid with steps along the z and θ coordinates of $h = 0.1$ and $d = 6°$, respectively, was used in the calculations. The calculations were continued until at all points of the grid the modulus of the difference of the computed quantities obtained in two successive iterations became less than 10^{-4}. Then the density gradient, which as follows from Eq. (1.3), is proportional to the flow of charged particles on the probe, was calculated at each point of the grid lying on the surface of the cylinder. The total current on the probe was found by integrating over the contour of the cylinder. The calculations were performed on a BÉSM-6 computer.

The convergence and stability of the difference scheme employed were checked in test calculations on a model problem of flow of an ideal liquid around a cylinder, for which the analytical expression for the saturation currents is known [4]. The calculations showed that the values of the total saturation currents obtained from the solution of the difference problem differ from those determined from the analytical expression [4] with $\mathrm{Re}_e \leq 5$ by not more than 1%.

The distributions of the velocities u_r and u_θ of viscous fluid flow around the cylinder were calculated in the range of gas-dynamic Reynolds numbers from 1 to 15, for which the flow

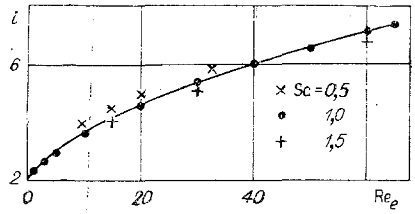

Fig. 3

around a cylinder is stationary [7]. A grid consisting of 31 to 36 points in the variable z, depending on Re, was employed. Increasing the number of points over the value indicated, i.e., locating the outer boundary farther away, has virtually no effect on the computed values of the saturation current.

The electric and gas-dynamic Reynolds numbers, as is well known, are related through the Schmidt number Sc by the relation $Re_e = ReSc$ ($Sc = \nu/D_i$, where ν is the kinematic coefficient of viscosity). Under real conditions Sc is of the order of unity. The saturation current was calculated, using the velocity distributions found, for Sc = 0.5, 1, and 1.5. The number of computed points along the z axis depended on Re_e and ranged from 36 at $Re_e = 1$ up to 12 at $Re_e = 15$. For $Re_e > 10$, owing to the fact that the outer boundary is located nearby, the saturation current could be calculated with a step equal to 0.05. The corresponding values of the velocities at the intermediate nodes of the grid were found by linear interpolation. Changing the integration step did not significantly affect the saturation current.

Figure 1 shows the results of calculations of the desnity j of the saturation ion current along the contour of the cylinder. One can see that under the flow conditions studied the back surface of the cylinder $0 \leq \theta \leq 90°$ also makes a significant contribution to the integral current. The relative magnitude of this contribution, compared with the front surface, $90° \leq \theta \leq 180°$, gradually decreases as Re increases. The increase in the current in the range $0 \leq \theta \leq 35°$ at Re = 15 is due to the development of a turbulent zone at the back surface of the cylinder.

Figure 2 shows the computed dependences of the dimensionless integral saturation current in on Re_e. One can see that the saturation current is virtually independent of Sc. The figure also shows, for comparison, the analytical dependences taken from [4] for model cases of uniform undistributed flow (broken line) and the velocity distribution of flow of an ideal liquid (dot-dash curve) of flow around the cylinder. Taking into account the real flow of viscous gas around the cylinder results in a slower increase of the saturation current as Re_e increases.

The computed dependences of the dimensionless saturation current on Re_e can be approximated well by a power-law function

$$i = a\mathrm{Re}_e{}^b, \tag{2.2}$$

where for Sc = 1, a = 0.43, and b = 0.42.

The relation

$$I_i = 4\pi e N_\infty D_i L i \tag{2.3}$$

(e is the electron charge) relates the dimensional current with the dimensionless current.

3. The saturation current on a spherical probe was determined analogously to the cylindrical case in Sec. 2. The calculation of the velocity field for flow of viscous gas around a sphere was performed by the method of [8] for Reynolds numbers $1 \leq Re \leq 65$, at which the flow around the sphere is stationary [7].

The equation for the quasineutral density of charged particles can be written in spherical coordinates as follows:

$$\frac{\partial^2 n}{\partial r^2} + \frac{2}{r}\frac{\partial n}{\partial r} + \frac{1}{r^2}\frac{\partial^2 n}{\partial \theta^2} + \frac{1}{r^2}\operatorname{ctg}\theta\frac{\partial n}{\partial \theta} - \frac{\mathrm{Re}_e}{2}\left(u_r\frac{\partial n}{\partial r} + u_\theta\frac{1}{r}\frac{\partial n}{\partial \theta}\right) = 0. \tag{3.1}$$

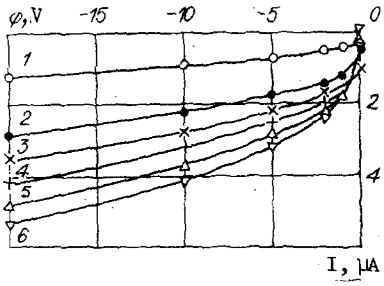

Fig. 4

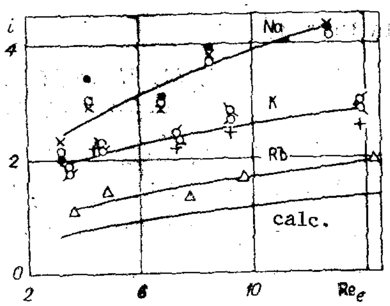

Fig. 5

After making the transformation $z = \ln r$ and constructing a finite-difference equation the problem can be solved by the method of successive approximations. The starting density was chosen as the density in the model case of a uniform undisturbed flow, found from Eq. (3.1) with $u_r = \cos\theta$ and $u_\theta = -\sin\theta$:

$$n = 1 - \exp(\varkappa r \cos\theta) \sum_{m=0}^{\infty} (-1)^m \frac{I_{m+1/2}(\varkappa)}{K_{m+1/2}(\varkappa)} (2m+1) \times \times \left(\frac{\pi}{2\varkappa r}\right)^{1/2} K_{m+1/2}(\varkappa r) P_m(\cos\theta). \tag{3.2}$$

Here $\varkappa = \mathrm{Re}_e/4$; $I_{m+1/2}$ and $K_{m+1/2}$ are Bessel functions of the first and second kind of half-integer order and imaginary arguments; and, $P_m(\cos\theta)$ are Legendre polynomials. Two terms were retained in the series (3.2) and $\mathrm{Re}_e = 1$.

The integral saturation current on the total surface of the sphere in the model case indicated is given by the expression

$$i = 2 - 2\pi \sum_{m=0}^{\infty} (-1)^m (2m+1) \frac{K'_{m+1/2}(\varkappa)}{K_{m+1/2}(\varkappa)} I^2_{m+1/2}(\varkappa), \tag{3.3}$$

which was employed to monitor the accuracy of the finite-difference calculations. The calculations showed that the difference between the saturation current, determined from the solution of the finite-difference problem and the formula (3.3), does not exceed 5% at Reynolds numbers $\mathrm{Re}_e \leq 40$.

The results of the calculation of the saturation current on a spherical probe in a viscous gas flow are presented in Fig. 3 in the form of a curve of the dimensionless current i versus Re_e. Based on the results presented we have a formula for determining the charged-particle density in the incident flow in a dimensional form:

$$I_i = 8\pi e D_i N_\infty R [1 + + 0.2(U_\infty R/D_i)^{0.62}]. \tag{3.4}$$

4. The formulas obtained were checked experimentally in an investigation of ionization in an acetylene–air flame with alkali additives. The experimental apparatus and the measurement procedure are described in [4]. The flame temperature was equal to 2370 ± 10 K and the flow velocity U_∞ = 4.4 ± 0.5 m/sec.

Water solutions of sodium, potassium, and rubidium salts with several concentrations were introduced into the flame. The concentration n_a of free atoms of these metals in the flame was determined by the method of the integral absorption coefficient of a spectral line [9]. The equilibrium values of the electron density n_e in the plasma flame were calculated with the help of Saha's equation from the values of the flame temperature and the measured value of n_a: for sodium $n_e = (2.3\text{-}4.1)\cdot 10^{10}$ with $n_a = (1.6\text{-}5.4)\cdot 10^{11}$ cm^{-3}, for potassium $n_e = (0.9\text{-}2.0)\cdot 10^{11}$ cm^{-3} with $n_a = (0.9\text{-}2.6)\cdot 10^{11}$ cm^{-3}, and for rubidium $n_e = 1.5\cdot 10^{11}$ cm^{-3} with $n_a = 6.3\cdot 10^{10}$ cm^{-3}.

Uncooled cylindrical probes with length L = 9 mm and different diameters as well as a spherical probe 2 mm in diameter were used in the experiments. The typical I-V curves are presented in Fig. 4, where the electric potential φ of the probes relative to the reference electrode is plotted along the abscissa axis; the body of the burner was used as the reference electrode. Curve 1 refers to the spherical probe and curves 2-6 refer to the cylindrical probe with diameters 0.75, 1, 1.6, 2, and 3 mm, respectively. The characteristics presented were obtained in a flame with potassium additive with $n_a = 9\cdot 10^{10}$ cm^{-3}.

It follows from the I–V curves of the spherical [10] and flat [1] probes in a stationary plasma that the start of the saturation ion current is realized with a dimensionless electric potential $\chi_p = e\varphi_p/kT_e \simeq -10$, where φ_p is the potential of the probe relative to the potential of the plasma, k is Boltzmann's constant, and T_e is the electron temperature. The measurements showed that the potential of the plama flame was equal to ~0.5 V. According to what was said above, the current with φ = –2 V was taken as the saturation ion current corresponding to the computed current given by Eq. (2.3) and Eq. (3.4).

In determining the charged-particle density from the formulas (2.3) and (3.4) the diffusion coefficient of sodium ions D_i = 5.2 cm^2/sec was employed [11]. Based on the data of [12] we obtained D_i = 4.8 cm^2/sec for potassium ions and D_i = 4.6 cm^2/sec for rubidium ions.

The experimental results obtained with the cylindrical probes are presented in Fig. 5. The charged-particle density calculated from Saha's equation based on spectral measurements was used to determine the dimensionless current i. The experimental points for each alkali element are described well by the power-law dependence (2.2) with the least-square values of the constants (a = 1.51 and b = 0.41 for sodium, a = 1.34 and b = 0.29 for potassium, and a = 0.78 and b = 0.37 for rubidium). Thus in the case of sodium and rubidium additives the exponent b is close to the computed value, but for all three elements the experimentally determined saturation current is somewhat higher than the theoretical value: on the average by a factor of 3.5 for sodium, a factor of 2.4 for potassium, and a factor of 1.5 for rubidium, i.e., the values of the charged-particle densities determined from the formula (2.3) are correspondingly greater by the factor indicated than the values computed based on the spectral measurements.

The measurements performed by the spherical probe gave analogous results. The densities found with the help of the formula (3.4) were 2.5 times greater for sodium, 1.8 times greater for potassium, and 1.2 times greater for rubidium than the values computed from the spectral measurements. The somewhat better agreement is explained by the smaller effective sorbing surface of the probe owing to the effect of the holder, which prevents charged particles from reaching part of the side surface of the sphere.

Thus the experimental results presented indicate that the expressions (2.3) and (3.4) obtained in this work describe quite satisfactorily the relation between the ion saturation current on the probe and the charged-particle density in the plasma of the flame. The observed discrepancies between the values of the density determined from probe measurements based on the formulas (2.3) and (3.4) and based on spectral measurements are evidently explained by the fact that the theoretical model used to calculate the saturation current neglects some processes occurring in the plasma, for example, formation of negative ions on the surface of the probe that is colder than the surrounding medium [13].

LITERATURE CITED

1. M. S. Benilov and G. A. Tirskiĭ, "On saturation currents in a dense plasma," Zh. Prikl. Mekh. Tekh. Fiz., No. 6 (1979).
2. M. S. Benilov, B. V. Rogov, and G. A. Tirskiĭ, "Theoretical determination of the ion saturation current on electric probes in subsonic plasma flows," Teplofiz. Vys. Temp., 19, No. 5 (1981).
3. M. S. Benilov, B. V. Rogov, and G. A. Tirskiĭ, "On the ion saturation current on an electric probe in a slowly moving plasma," Zh. Prikl. Mekh. Tekh. Fiz., No. 3 (1982).
4. Z. M. Egorova, A. V. Kashevarov, E. M. Fomina, and N. S. Tskhaĭ, "On measurement of the charged-particle density with a cylindrical Langmuir probe in the plasma of a flame," Teplofiz. Vys. Temp., 26, No. 3 (1988).
5. A. E. Hamielec and J. D. Raal, "Numerical studies of viscous flow around circular cylinders," Phys. Fluids, 12, No. 1 (1969).
6. P. P. Koryavov and Yu. P. Pavlovskiĭ, "Numerical solution of the problem of the motion of a circular cylinder in the flow of a viscous liquid," in: Problems in Applied Mathematics and Mechanics [in Russian], Nauka, Moscow (1971).
7. M. van Dyke, Perturbation Methods in Fluid Mechanics, Academic Press, New York (1964).
8. Y. Rimon and S. I. Cheng, "Numerical solution of a uniform flow over a sphere at intermediate Reynolds numbers," Phys. Fluids, 12, No. 5, Part 1 (1969).
9. Z. M. Egorova, A. V. Kashevarov, E. M. Fomina, and N. S. Tskhaĭ, "Determination of the concentration of alkali metal atoms in a hydrocarbon flame," Zh. Prikl. Spektrosk., 48, No. 6 (1988).
10. P. Chung, L. Talbot, and K. Turian, Electric Probes in Stationary and Flowing Plasmas, Springer-Verlag, New York (1975).
11. W. G. Mallard and K. S. Smyth, "Mobility measurements of atomic ions in flame using laser-enhanced ionization," Comb. Flame, 44, No. 1 (1982).
12. H. W. Ellis, "Transport properties of gaseous ions over a wide energy range," Atom. Data 2nd Nucl. Data Tables, 17, No. 3 (1976).
13. M. S. Benilov, V. F. Kosov, B. V. Rogov, and V. A. Sinel'shchikov, "Saturation currents on electric probes in flows of chemically reacting plasma with different types of ions," Teplofiz. Vys. Temp., 25, No. 3 (1987).